JOURNAL OF VIROLOGY, July 2010, p. 7140–7150 Vol. 84, No. 14
0022-538X/10/$12.00 doi:10.1128/JVI.00023-10
Copyright © 2010, American Society for Microbiology. All Rights Reserved.

Pepscan Mapping of Viral Hemorrhagic Septicemia Virus Glycoprotein G Major Lineal Determinants Implicated in Triggering Host Cell Antiviral Responses Mediated by Type I Interferon▽

V. Chico,[1] A. Martinez-Lopez,[1] M. Ortega-Villaizan,[1] A. Falco,[1] L. Perez,[1] J. M. Coll,[2] and A. Estepa[1]*

IBMC, Miguel Hernández University, 03202 Elche, Spain,[1] and INIA-SIGT, Departmento Biotecnología, 28040 Madrid, Spain[2]

Received 6 January 2010/Accepted 5 May 2010

Surface glycoproteins of enveloped virus are potent elicitors of type I interferon (IFN)-mediated antiviral responses in a way that may be independent of the well-studied genome-mediated route. However, the viral glycoprotein determinants responsible for initiating the IFN response remain unidentified. In this study, we have used a collection of 60 synthetic 20-mer overlapping peptides (pepscan) spanning the full length of glycoprotein G (gpG) of viral hemorrhagic septicemia virus (VHSV) to investigate what regions of this protein are implicated in triggering the type I IFN-associated immune responses. Briefly, two regions with ability to increase severalfold the basal expression level of the IFN-stimulated *mx* gene and to restrict the spread of virus among responder cells were mapped to amino acid residues 280 to 310 and 340 to 370 of the gpG protein of VHSV. In addition, the results obtained suggest that an interaction between VHSV gpG and integrins might trigger the host IFN-mediated antiviral response after VHSV infection. Since it is known that type I IFN plays an important role in determining/modulating the protective-antigen-specific immune responses, the identification of viral glycoprotein determinants directly implicated in the type I IFN induction might be of special interest for designing new adjuvants and/or more-efficient and cost-effective viral vaccines as well as for improving our knowledge on how to stimulate the innate immune system.

Type I interferons (IFN-α/ß) are a group of inducible cytokines that have a central role in innate antiviral immune responses because they establish an intracellular antiviral state (71) that prevents virus replication and restricts the spread of virus to neighboring cells (54, 61, 72). Binding of type I IFNs to their cellular receptors induces different cell signaling pathways leading to the transcription of specific sets of interferon-stimulated genes (ISGs), including those encoding important mediators of the antiviral response. The best-characterized ISGs encode the double-stranded-RNA (dsRNA)-dependent protein kinase R (PKR) protein (33, 67), the 2′-5′ oligoadenylate synthase (OAS) proteins (37, 41), and the myxovirus resistance proteins (Mx proteins) (5, 38, 70).

To date, most of the studies related to the induction of type I IFN-mediated responses by viruses have been focused on viral genomes and replication intermediates as the stimulus for these responses (68). However, additional viral ligands, such as envelope glycoproteins (gp's), viral glycolipids, and tegument, capsid, or nuclear proteins should be able to induce type I IFN production (68) since many cell types are able to mount a type I IFN-mediated antiviral response to physically and chemically inactivated virus as well as to fixed virus-infected cells (32, 42, 56).

IFN-inducing activity has been described for both soluble and transfected viral gp's from several RNA and DNA viruses, such as Sendai virus (66), type 4A human parainfluenza virus (HPIV-4A) (42), transmissible gastroenteritis coronavirus (TGEV) (17), herpes simplex virus type 1 (HSV-1) (3), human cytomegalovirus (CMV) (8, 11), influenza virus (56), human immunodeficiency virus type 1 (HIV-1) (25), and several members of the *Rhabdoviridae* family, including the mammalian rhabdovirus of vesicular stomatitis virus (VSV) (36) and the fish rhabdoviruses of infectious hematopoietic necrosis virus (IHNV) and viral hemorrhagic septicemia virus (VHSV) (10, 19, 43, 47, 48, 55, 77). Overall, IFN induction by viral gp's appears to result from their interactions with the surfaces of the type I IFN-producing cells (30, 32). However, neither the surface cell molecules nor the determinants on virus gp's that interact and initiate host IFN-mediated antiviral response have been identified so far.

A direct role for the envelope gpG proteins of VHSV and IHNV in type I IFN induction has been shown by the fact that fish immunized with a plasmid carrying the VHSV gpG or IHNV gpG gene showed strong upregulation of the IFN-α gene as well as of the several members of the ISG family (the *mx*, *irf3*, and *vig1* genes) (10, 19, 43, 47, 48, 55, 73). Moreover, *in vitro* cell transfection assays using virus-neutralizing monoclonal antibodies (MAbs) to VHSV gpG have suggested that the expression of the gpG protein on the surfaces of the transfected cells was more important in the induction of IFN than the viral gpG gene transcript expressed inside the transfected cells (1).

In this context, we have used in this study a collection of 60 synthetic 20-mer peptides (pepscan) overlapping by 10 amino acids (aa) and spanning the full length of the VHSV gpG protein to identify the VHSV gpG lineal determinants recognized by the responder cells to initiate the type I IFN-mediated

* Corresponding author. Mailing address: IBMC, Miguel Hernández University, Av. del Ferrocarril s/n, 03202 Elche, Spain. Phone: 34-96-6658436. Fax: 34-96-6658758. E-mail: a.estepa@umh.es.

▽ Published ahead of print on 12 May 2010.

antiviral response. We showed that short protein segments of VHSV gpG are able to increase severalfold the basal expression level of the trout interferon-stimulated (IS) *mx3* gene and to protect the responder cells against VHSV infection. In addition, the results obtained suggest that an interaction between VHSV gpG and integrins might be underlying the triggering of host IFN-mediated antiviral response.

Since (i) fish rhabdoviral infections, such as those caused by VHSV, are still a negative economic and social impact on aquaculture, (ii) DNA vaccination with a plasmid encoding rhabdovirus gpG seems the most adequate method for controlling those fish viral diseases, and (iii) the protection afforded by a VHSV DNA vaccine correlated with the ability of VHSV gpG to induce a strong type I IFN-related immune response, the identification of VHSV gpG determinants implicated on type I IFN-mediated response might be of definitive interest for designing new adjuvants and/or more-efficient and cost-effective viral vaccines as well as for improving our knowledge on how to stimulate the innate immune system.

MATERIALS AND METHODS

Cell cultures and virus. The fish cell lines EPC (epithelioma papulosum cyprinid) (31) and RTG-2 (fibroblastic cell line derived from rainbow trout gonad) (80), both purchased from the American Type Culture Collection (ATCC CRL-2872 and ATCC CCL-55, respectively), were used in this work. Recently, the ATCC has revealed that the EPC cell line, originally deposited as a carp (*Cyprinus carpio*) cell line, is in fact a fathead minnow (*Pimephales promelas*) cell line.

EPC cells were maintained at 28°C in a 5% CO_2 atmosphere with RPMI 1640 Dutch modified cell culture medium (Gibco, Invitrogen Corporation, United Kingdom) containing 10% fetal calf serum (FCS) (Sigma Chemical Co., St. Louis, MO), 1 mM pyruvate (Gibco, Invitrogen Corporation, United Kingdom), 2 mM glutamine (Gibco), 50 μg/ml gentamicin (Gibco), and 2 μg/ml amphotericin B (Fungizone). Likewise, RTG-2 cells were maintained at 20°C in a 5% CO_2 atmosphere with minimal essential medium (MEM) (with Earle's salts) cell culture medium (Gibco) containing 10% FCS (Sigma), 2 mM glutamine (Gibco), and 50 μg/ml neomycin sulfonate (Sigma).

Viral hemorrhagic septicemia virus strain 07.71 ($VHSV_{07.71}$), isolated in France from rainbow trout (*Oncorhynchus mykiss*) (24), was propagated in EPC cells at 14°C as previously reported (4). Supernatants from $VHSV_{07.71}$-infected EPC cell monolayers were clarified by centrifugation at 4,000 × *g* for 30 min and kept in aliquots at −70°C. Clarified supernatants were used for the experiments. The virus stock was titrated in 96-well plates by use of a previously developed immunostaining focus assay (focus-forming units [FFU]) (29, 49, 52).

Synthetic peptides from the sequence of glycoprotein G (gpG) of VHSV (VHSV gpG pepscan). Synthesis of 20-mer peptides overlapping by 10 amino acids and spanning the cDNA-derived amino acid sequence of the gpG protein of $VHSV_{07.71}$ (74) (GenBank accession number A10182) was performed by Chiron Mimotopes (Victoria, Australia). The pepscan peptides (Table 1) were named by a number corresponding to the position of their middle amino acid (10th position) in the gpG protein. The peptides were diluted in water at a final concentration of 1 mg/ml. VHSV gpG peptides (Table 2) p30, p31, p32, and p33 were synthesized by Genscript (Piscataway, NJ), and the mature sequence of winter flounder pleurocidin (WF-Ple) (GWGSFFKKAAHVGKHVGKAALTHYL) (15) was sequenced by Diverdrugs (Diverdrugs S.A., Barcelona, Spain). The peptide p9 (from VHSV gpG amino acid residues 56 to 81), employed in previous studies related to VHSV gpG (27), was also used.

Generation of a permanently transformed EPC cell culture expressing the gpG protein of VHSV. An EPC cell line enriched in cells stably expressing the gpG protein of VHSV (EPC-gpG cells) was obtained as previously described (12, 29), with minor modifications. Briefly, EPC cell monolayers grown in six-well plates were cotransfected with 1.5 μg of the pAE6-gpG (19) plasmid construct plus 0.5 μg of the pAE6-*pac* (puromycin resistance gene) plasmid construct and incubated for 48 h at 20°C. After the incubation period, puromycin-resistant cells were selected by adding 20 μg/ml of puromycin (Sigma) to the cell culture medium for 6 days. Resulting puromycin-resistant cells were seeded in 96-well plates at different densities and grown in cell culture medium conditioned by the growth of nontransfected EPC cells to favor the growth of isolated cells. Three days later, the wells were screened for the presence of surface VHSV gpG-expressing cells (cells expressing VHSV gpG on the membrane) by immunofluorescence (IF) using a cocktail of anti-gpG MAbs as described below. After 2 weeks, puromycin-resistant colonies were transferred to wells of 48-well plates and grown in conditioned medium (CM) supplemented with puromycin. Several

TABLE 1. Sequences and positions of the pepscan peptides in the sequence of VHSV gpG

Pepscan peptide no.	Sequence to C terminus
10	MEWNTFFLVILIIIIKSTTP
20	LIIIIKSTTPQITQRPPVEN
30	QITQRPPVENISTYHADWDT
40	ISTYHADWDTPLYTHPSNCR
50	PLYTHPSNCRDDSFVPIRPA
60	DDSFVPIRPAQLRCPHEFED
70	QLRCPHEFEDINKGLVSVPT
80	INKGLVSVPTRIIHLPLSVT
90	RIIHLPLSVTSVSAVASGHY
100	SVSAVASGHYLHRVTYRVTC
110	LHRVTYRVTCSTSFFGGQTI
120	STSFFGGQTIEKTILEAKLS
130	EKTILEAKLSRQEATDEASK
140	RQEATDEASKDHEYPFFPEP
150	DHEYPFFPEPSCIWMKNNVH
160	SCIWMKNNVHKDITHYYKTP
170	KDITHYYKTPKTVSVDLYSR
180	KTVSVDLYSRKFLNPDFIEG
190	KFLNPDFIEGVCTTSPCQTH
200	VCTTSPCQTHWQGVYWVGAT
210	WQGVYWVGATPKAHCPTSET
220	PKAHCPTSETLEGHLFIRTH
230	LEGHLFIRTHDHRVVKAIVA
240	DHRVVKAIVAGHHPWGLTMA
250	GHHPWGLTMACTVTFCGTEW
260	CTVTFCGTEWIKTDLGDLIQ
270	IKTDLGDLIQVTGPGGTRKL
280	VTGPGGTRKLTPNKCVNTDI
290	TPNKCVNTDIQMRGATDDFS
300	QMRGATDDFSYLNHLITNMA
310	YLNHLITNMAQRTECLDAHS
320	QRTECLDAHSDITASGKVSS
330	DITASGKVSSFLLSKFRPSH
340	FLLSKFRPSHPGPGKAHYLL
350	PGPGKAHYLLDGQIMRGDCD
360	DGQIMRGDCDYEAVVSINYN
370	YEAVVSINYNRAQYKTMNNT
380	RAQYKTMNNTWKSWKRVDNN
390	WKSWKRVDNNTDGYDGMIFG
400	TDGYDGMIFGDKLIIPDIEK
410	DKLIIPDIEKYQSVYDSGML
420	YQSVYDSGMLVQRNLVEVPH
430	VQRNLVEVPHLSIVFVSNTS
440	LSIVFVSNTSDLSTNHIHTN
450	DLSTNHIHTNLIPSDWSFNW
460	LIPSDWSFNWSLWPSLSGMG
470	SLWPSLSGMGVVGGAFLLLV
480	VVGGAFLLLVLCCCCKASPP
490	LCCCCKASPPIPNYGIPMQQ
500	SPPIPNYGIPMQQFSRSQTV

TABLE 2. Sequences and positions of the designed synthetic peptides in the sequence of VHSV gpG

Peptide name	Sequence to C terminus	Position (aa)[a]
p9[b]	RPAQLRCPHEFEDINKGLVSVPT	58–80
p30	LIQVTGPGGTRKLTP	268–282
p31	LTPNKCVNTDIQMRGATDDFSYLNH LITNMA	280–310
p32	SHPGPGKAHYLLDGQ	339–353
p33	HPGPGKAHYLLDGQIMRGDCDYEA VVSINYN	340–370

[a] The numbers correspond to the amino acid positions in the gpG protein from VHSV $_{07.71}$ (75), including the signal peptide.
[b] p9 was previously described (27).

EPC cell cultures enriched in VHSV gpG protein-expressing cells were obtained, and one of them was selected for further work. The selected EPC-gpG cell line was grown in 96-well plates and gradually transferred into cell culture flasks. The EPC-gpG cell line has been maintained by continuous culture (about one subculture per week) in the presence of 10 μg/ml of puromycin at 20°C for more than 1 year.

Induction of trout *mx3* gene expression by fixed EPC-gpG cells. Both EPC and EPC-gpG cells, grown in 25-cm^2 culture flasks, were detached using Ca^{2+}- and Mg^{2+}-free phosphate-buffered saline (PBS), washed, counted, fixed with 4% paraformaldehyde in PBS (15 min at room temperature), and then dispensed into 24-well plates containing RTG-2 cell monolayers ($\sim 2 \times 10^5$ cells per well) at different EPC/RTG-2 ratios (from 1/5 to 1/50). After overnight incubation at 20°C, RTG-2 cells were either collected for total RNA extraction or fixed with cold methanol for IF assays. The expression of the trout *mx3* gene was then assessed at the transcription and protein levels by quantitative reverse transcription-PCR (RT-qPCR) and IF, respectively, as indicated below.

Induction of trout *mx3* gene expression by poly(I:C) and VHSV gpG peptides. RTG-2 cells grown in 48-well plates were treated with 3 μg/ml of each of the gpG pepscan peptides, with different concentrations (from 1 to 12 μg/ml) of the peptides p9 (aa 56 to 81) (27), p30, p31, p32, and p33 (Table 2), or with 40 μg/ml of poly(I:C) as a positive control, at 20°C for 24 h. In addition, peptide mixtures containing p31 and p33, each at 1, 2, 3, or 6 μg/ml, were also used. As a negative control, RTG-2 cell monolayers were treated or not treated with WF-Ple, an antimicrobial peptide (AMP) from flatfish that does not affect the expression levels of genes associated with the IFN response (21, 28).

In all cases, after the incubation period, the medium was removed, cells were detached with Ca^{2+}- and Mg^{2+}-free PBS, total RNA was extracted, and the expression of the trout *mx3* gene was evaluated by RT-qPCR.

Production of anti-trout Mx sera in rabbit. The 15-mer peptide corresponding to amino acid residues 209 to 223 of the rainbow trout Mx3 protein (GenBank accession number U47946) was synthesized by Sigma to a purity of >95%, as determined by high-performance liquid chromatography and mass spectrophotometry. To obtain the antisera, rabbits were first injected with 1 mg/ml of synthetic peptide diluted 1:1 in Freund's complete adjuvant. Four weeks later, a second injection with the same antigen in Freund's incomplete adjuvant was given. Blood samples were collected before injection (preimmune sera) and 20 days after the second injection. The blood samples were then incubated for 2 h at 4°C and centrifuged to obtain the sera.

Detection of the VHSV gpG and trout Mx proteins by IF. To detect the presence of VHSV gpG on the cell membranes, EPC-gpG cells grown in 24-well plates were fixed with 4% paraformaldehyde in PBS (15 min at room temperature) and incubated with a cocktail of anti-gpG MAbs (53), including two conformational antibodies (MAbs 3F1A2 and C10) and one nonconformational (MAb I10) antibody (7, 35), diluted 200-fold for 2 h at room temperature. After a wash with PBS, 300 μl of fluorescein-labeled rabbit anti-mouse IgG Ab (Sigma) diluted 200-fold was added per well and the incubation was continued for 45 min.

To detect rainbow trout Mx3 protein, RTG-2 cells incubated in the presence of paraformaldehyde-fixed EPC-gpG cells were fixed with cold methanol (15 min at room temperature) and then incubated with the rabbit anti-trout Mx3 polyclonal serum diluted 200-fold in PBS at room temperature for 2 h. The indirect staining was carried out using a goat anti-rabbit antibody conjugated to rhodamine (Sigma). In all cases, stained cells were viewed and photographed with an inverted fluorescence microscope (Nikon Eclipse TE2000-U; Nikon Instruments, Inc., NY) provided with a digital camera (Nikon DS-1QM).

Preparation of CM from RTG-2 cell cultures. In order to prepare conditioned medium (CM), RTG-2 cells grown in 48-well plates were treated with the peptides p31 and p33 (6 μg/ml) or poly(I:C) as described above for 24 h. After extensive washes with PBS, 250 μl of fresh medium supplemented with 10% FCS was added to each well and plates were further incubated at 20°C for 24 h. Finally, the supernatants were collected and clarified by centrifugation at 800 × *g* for 10 min. Clarified supernatants were treated with 1 N HCl to reduce the pH to 2. After overnight incubation at 4°C, the samples were heated to 50°C for 60 min and the pH was restored to 7.6 by addition of 1 N NaOH. CM from supernatants of nontreated RTG-2 cells was also prepared.

Infection of RTG-2 cells with VHSV. RTG-2 cells treated with VHSV gpG peptides, poly(I:C), or WF-Ple as well as incubated with CM from RTG-2 cell cultures (diluted 1/5 to 1/125) treated as indicated above were washed extensively with PBS and infected with VHSV (multiplicity of infection [MOI] of 2×10^{-3}) in a final volume of 100 μl/well of culture medium supplemented with 2% FCS at 14°C for 2 h. The infected cell monolayers were then washed, fresh medium was added, and plates were further incubated for 24 h. VHSV replication in RTG-2 cells was evaluated by RT-qPCR using specific primer and probe sequences for the gene encoding the protein N of VHSV (Table 3). Nontreated RTG-2 cells infected with VHSV were included as a control.

RNA isolation and cDNA synthesis. An RNeasy Plus minikit (Qiagen, Hilden, Germany) was used for total RNA extraction in accordance with the manufacturer's instructions, and isolated RNAs were stored at −80°C until used. One microgram of RNA, as estimated by a NanoDrop 1000 spectrophotometer (Thermo Fisher Scientific, Inc.) was used to obtain the cDNA using Moloney murine leukemia virus (M-MLV) reverse transcriptase (Invitrogen) as previously described (29).

Quantitative PCR assays. Quantitative PCR (qPCR) in real time was performed using the ABI PRISM 7300 System (Applied Biosystems, NJ) as previously described (29). *mx3* gene-specific primer and probe sequences (Table 3) for RT-qPCR were designed from the rainbow trout *mx3* gene sequence (GenBank accession number U47946) to generate a single gene-specific amplicon of 88

TABLE 3. Sequences of primers and probes for RT-qPCR

Gene and orientation[a]	Sequence		Reference or GenBank accession no.
	Primer	Probe	
mx3			
Fw	5′-GGATGGTCTTGGTTTTTTTTCTTTT-3′	5′-TGTATTTTTTGGGAGGATAACA-3′	U47946
Rv	5′-CTGGGTCCACAGTGTACATTTAGTTG-3′		
N_{VHSV}			
Fw	5′-GACTCAACGGGACAGGAATGA-3′	5′-TGGGTTGTTCACCCAGGCCGC-3′	(18)
Rv	5′-GGGCAATGCCCAAGTTGTT-3′		
ef1-α[a]			
Fw	5′-ACCCTCCTCTTGGTCGTTTC-3′	5′-GCTGTGCGTGACATGAGGCA-3′	(60)
Rv	5′-TGATGACACCAACAGCAACA-3′		

[a] Fw, forward; Rv, reverse; *ef1*-α, elongation factor 1-α.

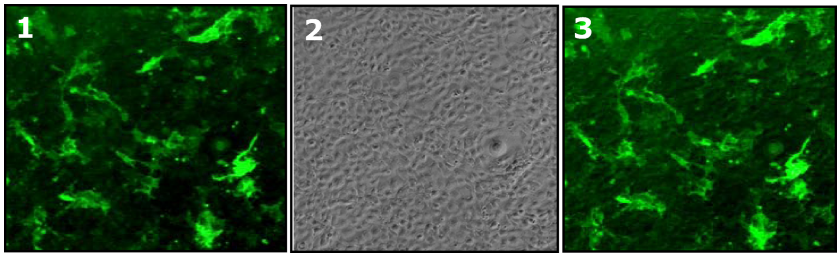

FIG. 1. Expression of VHSV gpG on the surfaces of EPC-gpG cells. Fresh EPC cell monolayers were cotransfected with the pAE6-gpG and pAE6-*pac* (puromycin resistance gene) plasmid constructs. After an incubation period in the presence of puromycin, the remaining cells were screened for the presence of surface VHSV gpG (cells expressing VHSV gpG on the membrane) by immunofluorescence (IF) using a cocktail of anti-G MAbs and fluorescein isothiocyanate (FITC)-labeled anti-mouse IgG Ab. Shown are EPC-gpG cell micrographs at fluorescent (field 1) and visible (field 2) light fields; field 3 is a merged image of fields 1 and 2.

nucleotides. Reactions were performed in a 20-μl volume comprising 2 μl of cDNA reaction mixture, 900 nM each primer, 200 nM probe, and 10 μl of TaqMan universal PCR master mix (Applied Biosystems). The cycling conditions were 50°C for 2 min and 95°C for 10 min, followed by 40 cycles at 95°C for 15 s and 60°C for 1 min. Gene expression results were analyzed by means of the $2^{-\Delta\Delta Ct}$ method (46), using as an endogenous control for quantification the cellular elongation factor 1 alpha (EF-α) gene (the primer and probe sequences are listed in Table 3) (60). The control cells (nontreated RTG-2 cells) served as the calibrator cells, and fold increases were calculated relative to the level for these cells.

To detect the N protein (pN) of VHSV, pN gene-specific primer and probe sequences (Table 3) under the conditions previously described (18, 20, 29) were used. The internal reference for normalization of data was the cellular 18S rRNA (Applied Biosystems).

Modeling of the 3D structure of VHSV gpG. Homology modeling for prediction of the tridimensional (3D) structure of VHSV gpG was performed using the Swiss-Model server (http://swissmodel.expasy.org/). Prefusion conformation of VSV gpG (63, 64) (Protein Data Bank [PDB] file code 2J6J) was used as a template structure. VHSV and VSV gpG alignment was performed using CLUSTAL W (76).

Statistical analysis. Statistical comparisons were made using a paired, two-tailed Student *t* test or analysis of variance (ANOVA) with a post hoc test (Tukey's).

RESULTS

Trout *mx3* gene expression induced by fixed EPC cells permanently expressing VHSV gpG. It has previously been reported that the expression of VHSV gpG on the surfaces of rainbow trout-transfected cells was important in the induction of type I IFN response rather than the viral VHSV gpG gene transcript expressed inside the transfected cells (1). To reinforce this outcome, type I IFN response in RTG-2 cells cultured in the presence of EPC-gpG cells (EPC cell line stably expressing VHSV gpG) was evaluated. For that, after the expression of VHSV gpG on the membranes of EPC-gpG cells was evaluated using a cocktail of anti-gpG MAbs (including conformational anti-gpG MAbs) by IF (Fig. 1), RTG-2 cells were coincubated with paraformaldehyde-fixed EPC or EPC-gpG cells and the expression of the IS *mx3* gene was assessed 24 h later, with transcription and protein levels determined by RT-qPCR and IF, respectively. The IS *mx* gene was chosen as a marker for IFN-mediated response because Mx proteins have proved to be a very specific and sensitive marker for type I IFN induction (39, 69, 79) and direct induction of this gene by rainbow trout type I IFN has been demonstrated (81). On the other hand, among the three different rainbow trout *mx* genes (*mx1*, *mx2*, and *mx3*), *mx3* was selected since it is the Mx protein isoform predominantly expressed in RTG-2 cells in response to different type I IFN inducers (73).

The presence of VHSV gpG on the membranes of paraformaldehyde-fixed EPC-gpG cells (Fig. 1) markedly increased the expression levels of Mx3 protein in terms of both transcription (Fig. 2A) and protein levels (Fig. 2B, lower panels) in RTG-2 cells, while only negligible accumulation of *mx3* transcripts (Fig. 2A) and expression of Mx3 protein (Fig. 2B, upper panels) were observed upon contact with paraformaldehyde-fixed EPC cells. A maximal induction level of ~14.000-fold was observed at a paraformaldehyde-fixed EPC-gpG cell/RTG-2 cell ratio of 1/40 (Fig. 2A).

Trout *mx3* gene expression induced by the 20-mer peptides from the VHSV gpG pepscan. Having established that the contact between VHSV gpG and the surfaces of RTG-2 cells efficiently triggers the expression of the *mx3* gene, we asked whether specific segments of VHSV gpG suffice for initiating the type I IFN-mediated antiviral response. With this aim, RTG-2 cells were incubated with each of the 20-mer peptides from a pepscan set of 60 peptides spanning the entire sequence of gpG of $VHSV_{07.71}$ and then assayed for the presence of *mx3* gene transcripts. The results were compared to those observed for nontreated RTG-2 cells or RTG-2 cells treated with an irrelevant peptide (WF-Ple).

Overall, 9 of the 60 peptides from the VHSV gpG pepscan induced a significant upregulation of the *mx3* gene in peptide-treated RTG-2 cells relative to the level for control cells (untreated RTG-2 cells) (Fig. 3A). These 9 *mx3*-inducing peptides defined 4 separated regions located at the N-terminal, central, and C-terminal domains of gpG of VHSV (Fig. 3B). The region located at the N terminus of the protein (amino acids 50 to 90) (Fig. 3B, yellow) was defined by 3 overlapping peptides (p60, p70, and p80) that increased the presence of *mx3* gene transcripts 3- to 5-fold (~3.4-fold for p60, 4-fold for p70, and 5-fold for p80). However, certain variability in the response induced by these peptides was observed among different pepscan assays, as indicated by the high standard deviations (SD) (Fig. 3A). The second region (amino acids 280 to 310) (Fig. 3B, light green), which overlapped by 3 amino acids within the C-terminal sequence of the putative fibronectin binding site of the VHSV gpG protein (amino acids 268 to 282) (6), was defined by the pepscan peptides p290 and p300, which induced a 3- to 3.5-fold increase in *mx3* transcript expression (Fig. 3A). Very close to the second region, the 2 overlapping peptides

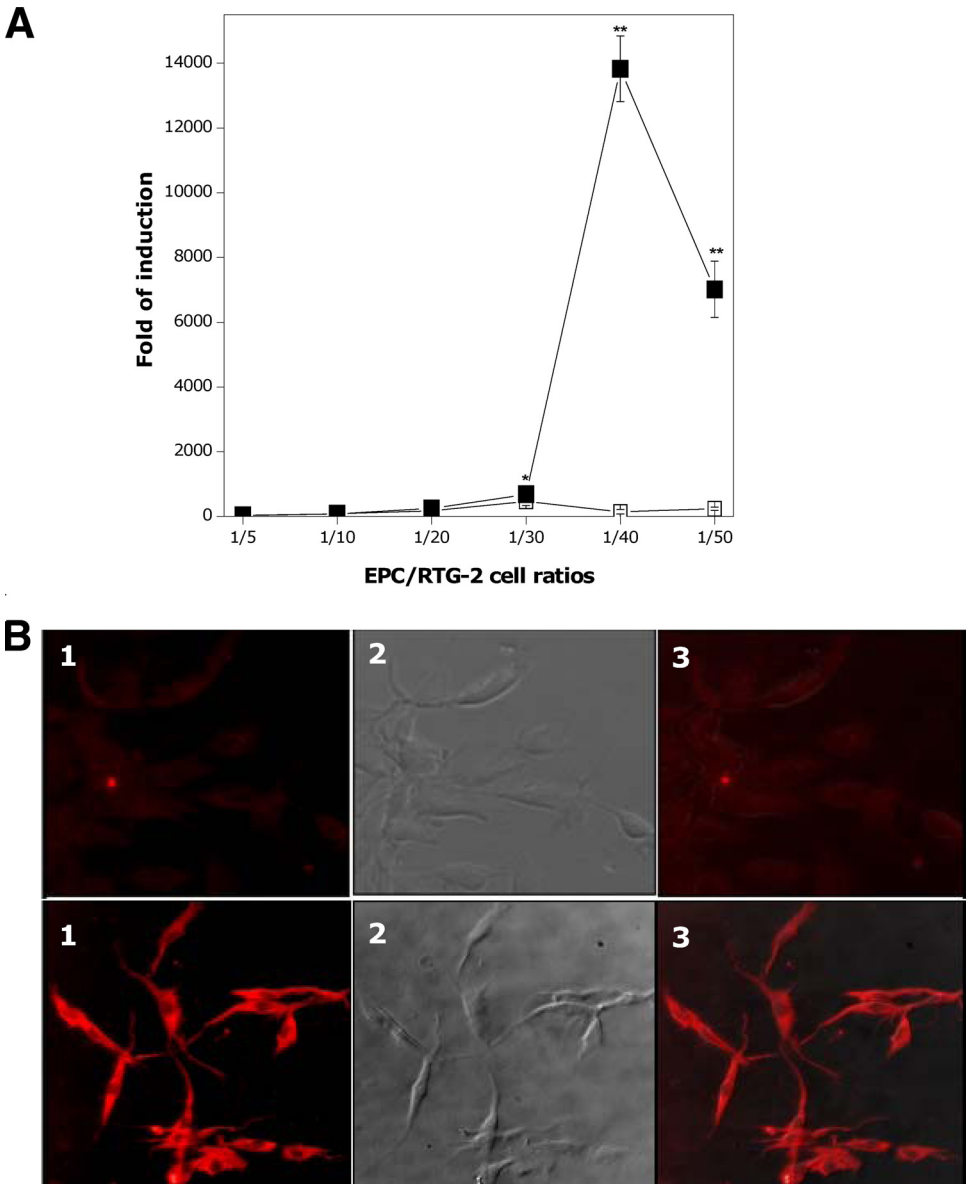

FIG. 2. *mx3* transcript (A) and protein (B) expression in RTG-2 cells coincubated with paraformaldehyde-fixed EPC-gpG cells. Fresh RTG-2 cells and paraformaldehyde-fixed EPC-gpG cells were cocultured at different ratios, and expression of *mx3* was assessed 24 h later both at transcriptional and protein levels by RT-qPCR and IF, respectively. (A) Fold changes in *mx3* gene expression assayed by RT-qPCR. Fold increases were calculated relative to the level for nontreated RTG-2 cells. Data are the mean fold changes ± SD for three independent experiments, each performed in duplicate. Asterisks indicate significant differences in *mx3* gene induction relative to the level for control cells at *P* values of <0.05 (*) and *P* values of <0.01 (**). ■, cells cocultured with paraformaldehyde-fixed EPC-gpG cells; □, cells cocultured with paraformaldehyde-fixed EPC cells. (B) RTG-2 cells cocultured with paraformaldehyde-fixed EPC-gpG (lower panel) or EPC cells (upper panel) at a 1/40 ratio and stained with an anti-Mx3 protein serum. Shown are RTG-2 cell micrographs at fluorescent (field 1) and visible (field 2) light fields; field 3 is a merged image of fields 1 and 2.

p350 (>6-fold) and p360 (>3-fold) identified another major IFN-inducing site (amino acids 340 to 370) in the VHSV gpG amino acid sequence (Fig. 3B, magenta). Curiously, important differences related to *mx3* gene expression levels were observed between both peptides since p350 induced an *mx3* transcript accumulation level twice as high as that induced by p360 (Fig. 3A). Finally, the fourth region (amino acids 461 to 490) was defined by the peptides p470 and p480 and included the transmembrane region of gpG (amino acids 472 to 492) (Fig. 3B, dark green). As expected, WF-Ple lacked the ability to significantly increase the *mx3* expression levels up to those observed in the control cells, while the highest levels of *mx3* transcripts (>4,000-fold) were induced by poly(I:C) (data not shown).

It is noteworthy that individual gpG pepscan peptide-mediated upregulation of the *mx3* gene (Fig. 3A) was modest (from 3- to 6-fold) compared to that elicited by the fixed cells expressing the gpG protein on the membrane (Fig. 2A), suggest-

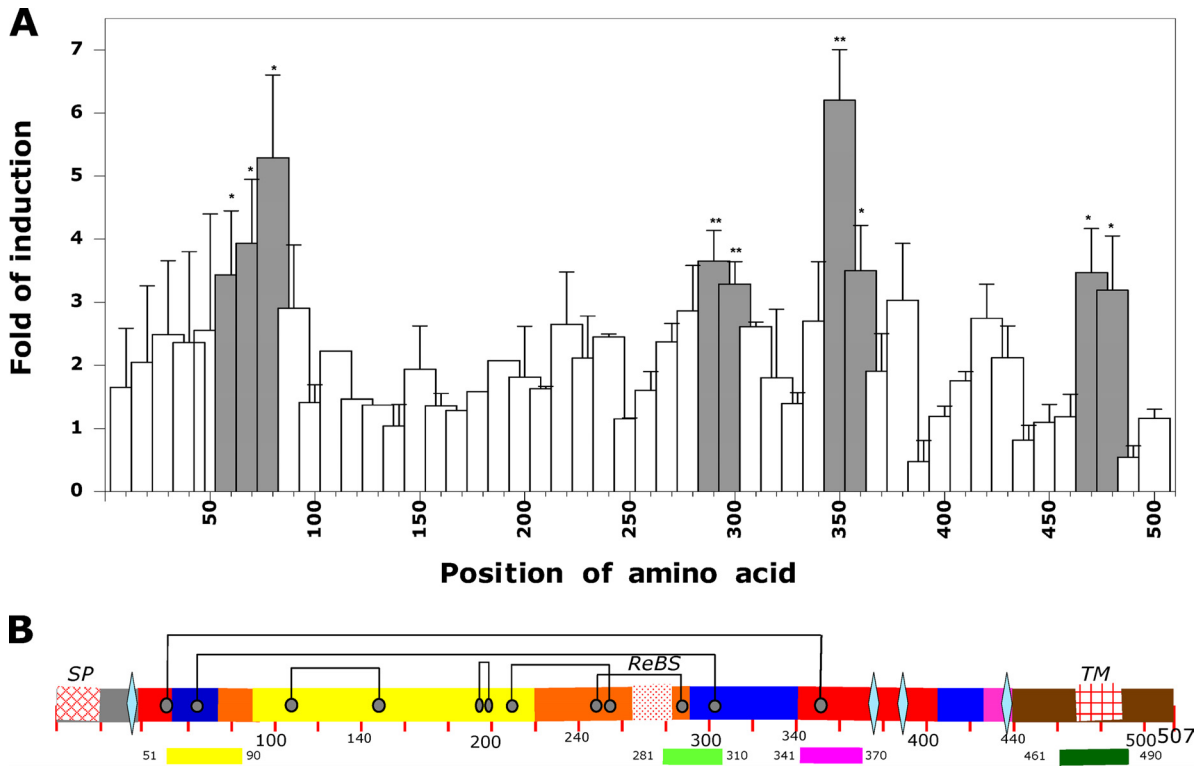

FIG. 3. Fold changes in the *mx3* gene expression in response to VHSV gpG synthetic 20-mer peptides assayed by real-time RT-qPCR (A) and schematic overview of VHSV gpG features plotted on a linear diagram (B). (A) Fresh RTG-2 cells, grown in 48-well plates, were incubated with 3 μg/ml of each of the peptides from the pepscan of 20-mer peptides. After 48 h of incubation at 20°C, total RNA was extracted and the expression of transcripts of *mx3* was estimated by RT-qPCR. Fold increases were calculated relative to the level for nontreated RTG-2 cells. Data are the mean fold changes ± SD for three independent experiments, each performed in duplicate. Gray bars indicate pepscan peptides that induced significant changes in *mx3* gene expression relative to the level for control cells at P values of <0.05 (*) and P values of <0.01 (**). (B) Sequence of the VHSV gpG protein colored by domains as their homologous counterparts of VSV gpG (63, 64). Red, domain I, or the lateral domain; blue, domain II, or the trimerization domain; orange, domain III, or the PH domain; yellow, domain IV, or the fusion domain. The filled diamond indicates the positions of the N-linked glycosylation sites (Asn30, Asn378, Asn389, and Asn438). SP, signal peptide (amino acids 1 to 20); TM, transmembrane region (amino acids 472 to 492); ReBs, putative receptor binding site (amino acids 268 to 282). Horizontal bars represent the *mx3*-inducing regions defined by the pepscan peptides p60, p70 and p80 (yellow), p290 and p300 (light green), p350 and p360 (magenta), and p470 and p480 (dark green).

ing that several peptides and/or the conformation of these peptides within the context of the entire protein structure might be needed for maximal *mx3* gene expression.

Trout *mx3* gene expression induced by synthetic peptides defined by the *mx3* inducing-pepscan peptides. To further confirm the role played by the VHSV gpG lineal regions mapped by pepscan in triggering the type I IFN-mediated antiviral responses, longer peptides (*mx3*-inducing peptides) spanning the amino acid sequence of three of the major VHSV gpG-*mx3*-inducing regions mapped (Fig. 3B) were assayed, except for the peptide covering p470 and p480, which included the transmembrane region of VHSV gpG because of their highly hydrophobic nature. Therefore, peptides p31 (residues 280 to 310) and p33 (residues 340 to 370), covering the complete amino acid sequence defined by the 20-mer overlapping peptides p290-p300 and p350-p360, respectively, were synthesized. For assaying the VHSV gpG region defined by the pepscan peptides p60 to p80, the so-called p9 peptide (residues 58 to 80), a peptide related to the fusion domain of VHSV gpG (14, 27), was employed.

Figure 4A shows that *mx3* gene expression was dose dependently induced by p31 and p33 with a maximal induction at a peptide concentration of 12 μg/ml. In contrast, no significant upregulation of the *mx3* gene by p9 was observed at any of the concentrations used (Fig. 4A), as expected from the variability in the response obtained among the different assays testing the pepscan peptides that defined this region (Fig. 3A). Regarding p31 and p33 combinations, a mild synergistic effect was detected when the peptide mixture was used at a very low concentration (≤2 μg/ml) (data not shown). However, when both peptides were mixed at higher concentrations, precipitates that precluded further test interpretation were formed because of the slightly hydrophobic nature of those peptides.

It is known that IFN induction can be initiated by binding of the viral glycoproteins to cellular virus entry receptors (2). Since fibronectin has been proposed as the main cellular receptor for VHSV (6), we also synthesized and tested for *mx3* gene induction a peptide, p30, containing the amino acid sequence of the putative fibronectin binding site of VHSV gpG (residues 268 to 282). Apparently, p30 failed to produce a remarkable induction of the *mx3* gene, but a 4-fold upregu-

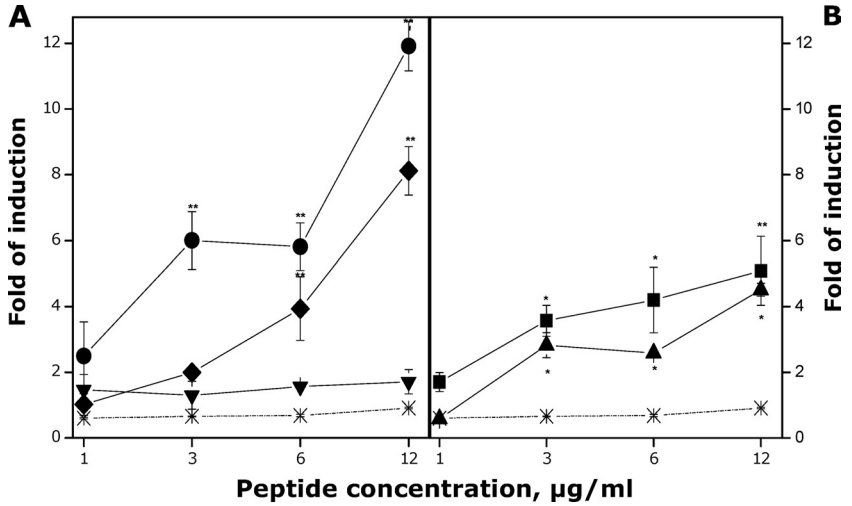

FIG. 4. Fold changes in the *mx3* gene expression in response to VHSV gpG regions selected from the pepscan (*mx3*-inducing peptides) assayed by RT-qPCR. RTG-2 cells were treated with different concentrations (from 1 to 12 μg/ml) of each of the *mx3*-inducing peptides (p9, p31, and p33 [A] and p30 and p33 [B]) or of WF-Ple for 48 h at 20°C. Total RNA was then extracted and *mx3* gene expression estimated by RT-qPCR. Fold increases were calculated relative to the level for nontreated RTG-2 cells. Data are the mean fold changes ± SD for three independent experiments, each performed in duplicate. As shown in panel A, p33 significantly increased the *mx3* gene expression at peptide concentrations of 3, 6, and 12 μg/ml while p9 and WF-Ple did not, and p31 caused significantly increased expression levels at the highest concentrations tested (6 and 12 μg/ml). Likewise, both p30 and p33 (B) significantly increased the *mx3* gene expression at peptide concentrations of 3, 6, and 12 μg/ml. *, $P < 0.05$; **, $P < 0.01$. Significant differences between the mean fold changes in *mx3* gene expression induced by p33 and p32 at 3, 6, and 12 μg/ml were also found by Tukey's test ($P < 0.05$). ▼, p9; ▲, p30; ◆, p31; ■, p32; ●, p33; X, WF-Ple.

lation was observed at a peptide concentration of 12 μg/ml (Fig. 4B).

On the other hand, p33, the *mx3*-inducing peptide that generated the highest levels of induction of the *mx3* gene at a peptide concentration of 12 μg/ml (≥11-fold) (Fig. 4A), contains an RGD motif in its sequence (residues 356 to 358) (Table 2). The tripeptide RGD motif is a paradigm of the integrin recognition sequence (65, 78), and it has been shown that several viruses use RGD-binding integrins as receptors or coreceptors (16). To investigate whether the RGD motif present in p33 was related to the *mx3* gene upregulation, p32 (residues 339 to 353), a peptide that is shorter than p33 and does not have the RGD sequence (Table 2), was also synthesized. We chose to delete the C terminus of p33 instead of mutating or eliminating the RGD sequence because the p33 peptide C terminus was included in the pepscan peptide p370 (Table 1) and no *mx3* gene upregulation was observed in response to this peptide (Fig. 3).

After treatment of the RTG-2 cells with p32, significant upregulation of the *mx3* gene relative to the level for control cells was observed at peptide concentrations of 3, 6, and 12 μg/ml (Fig. 4B), but this upregulation was significantly lower than that induced by p33 (Fig. 4A). Therefore, the RGD motif present in the sequence of VHSV gpG, and hence the cellular integrins, might play a key role, not previously identified, in triggering the host innate response after VHSV infection.

No significant induction of *mx3* gene expression was observed after the cells were treated with WF-Ple (Fig. 4), as was previously observed in the pepscan assays.

Resistance to VHSV infection of RTG-2 cells treated with VHSV gpG-*mx3*-inducing peptides. To determine whether the upregulation of the *mx3* gene in peptide-treated cells correlated with cellular resistance to VHSV infection, RTG-2 cells were preincubated with increasing concentrations (from 3 to 12 μg/ml) of the major VHSV gpG-*mx3* inducing peptides and VHSV infectivity was estimated 24 h later. As expected, VHSV-infected control cells (RTG-2 cells treated with WF-Ple or untreated) efficiently propagated the virus and produced ~100 VHSV-infected cell foci per well (data not shown). In contrast, RTG-2 cells treated with p31 (Fig. 5A) or p33 (Fig. 5B) showed significantly reduced susceptibility to VHSV since both peptides inhibited VHSV infectivity up to 50% except for p33 at 3 μg/ml. Minimal infectivity was observed when RTG-2 cells were preincubated prior to infection with 12 μg/ml of p31 (~25%) or p33 (~22%) (Fig. 5A and B). Peptides p30 (Fig. 5C) and p32 (Fig. 5D) were markedly less effective in reducing VHSV infectivity, and poly(I:C) completely abolished (100%) VHSV replication (data not shown). Moreover, the VHSV infectivity reductions caused by treatment of cells with p32 at 6 and 12 μg/ml were significantly inferior to those caused by treatment with p33 (Fig. 5B and D), which again suggests that the presence of the RGD motif seems to be important for p33 activity.

Taken together, these results seem to indicate that the regions of VHSV gpG defined by p31 and p33 induce in the cells a functional intracellular antiviral state that prevents VHSV replication and restricts the spread of virus among neighboring cells.

Resistance to VHSV infection of RTG-2 cells treated with CM from RTG-2 cells treated with VHSV gpG-*mx3*-inducing peptides. To exclude the possibility that RTG-2 cells could respond to *mx3*-inducing peptides by producing other cytokines/soluble antiviral factors, cell supernatants were analyzed for the presence of biologically active type I IFN by measuring their capacity to induce antiviral responses to VHSV in RTG-2 cells. Thus, conditioned medium (CM) from nontreated cells

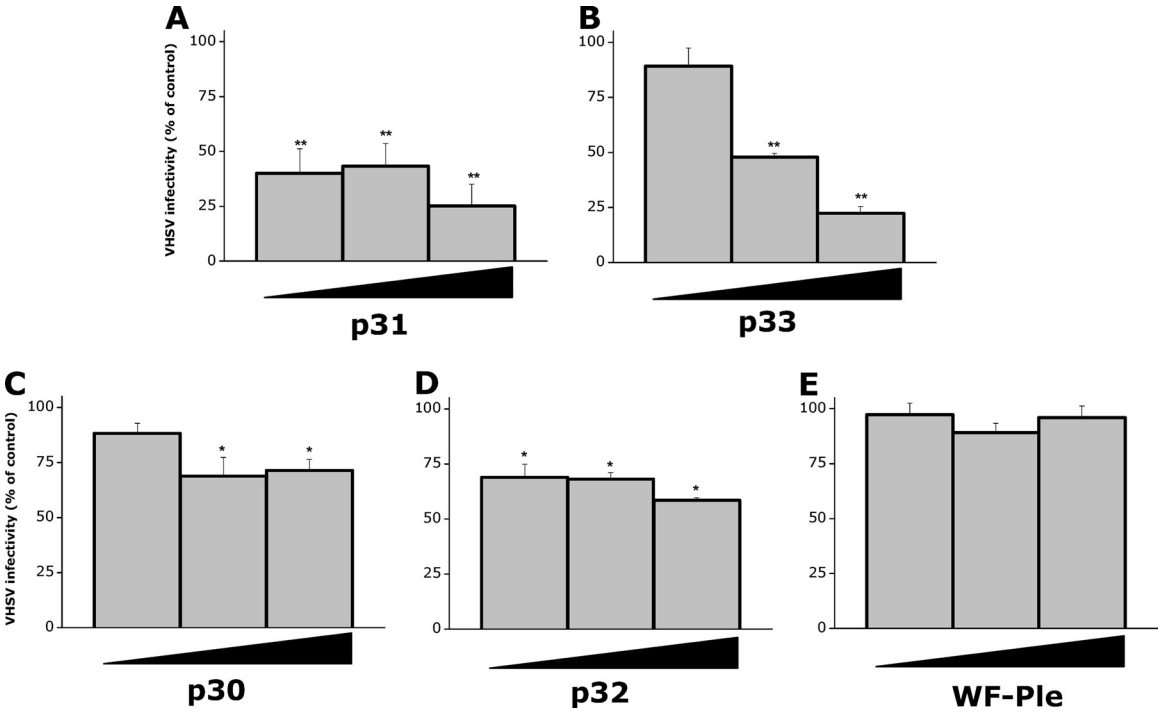

FIG. 5. Resistance to VHSV infection of RTG-2 cells treated with the *mx3*-inducing peptides. RTG-2 cells were treated with increasing concentrations (3, 6, and 12 μg/ml) of p31 (A), p33 (B), p30 (C), p32 (D), or WF-Ple (E) and then infected with VHSV (MOI of 2×10^{-3}) for 2 h at 14°C. After the unbound virus was washed, the infected cell monolayers were incubated for 24 h at 14°C and VHSV infectivity was estimated by RT-qPCR. Black triangles represent increasing peptide concentrations. The results are expressed as percentages of infectivity and calculated by the formula (VHSV infectivity in treated cells/VHSV infectivity in nontreated cells) × 100. Data are the mean percentages of infectivity ± SD for three independent experiments, each performed in triplicate. All *mx3*-inducing peptides significantly reduced the VHSV infectivity at all of the concentrations tested but 3 μg/ml for p30 and p33. *, $P < 0.05$; **, $P < 0.01$. Tukey's test ($P < 0.05$) also showed significant differences between the mean percentage of infectivity of the cells treated with p33 and that of the cells treated with p32 both at 6 and 12 μg/ml.

or poly(I:C)-, p31-, or p33-treated RTG-2 cells were prepared. Fresh RTG-2 cell monolayers were then incubated with these different CM for 24 h and, after extensive washing, infected with VHSV. As expected, the treatment of RTG-2 cells with CM from RTG-2 cells treated with poly(I:C) (Fig. 6A), p31 (Fig. 6B), or p33 (Fig. 6C) significantly conferred protection against VHSV infection. In contrast, nonsignificant protection was conferred by the CM from nontreated RTG-2 cells. In this

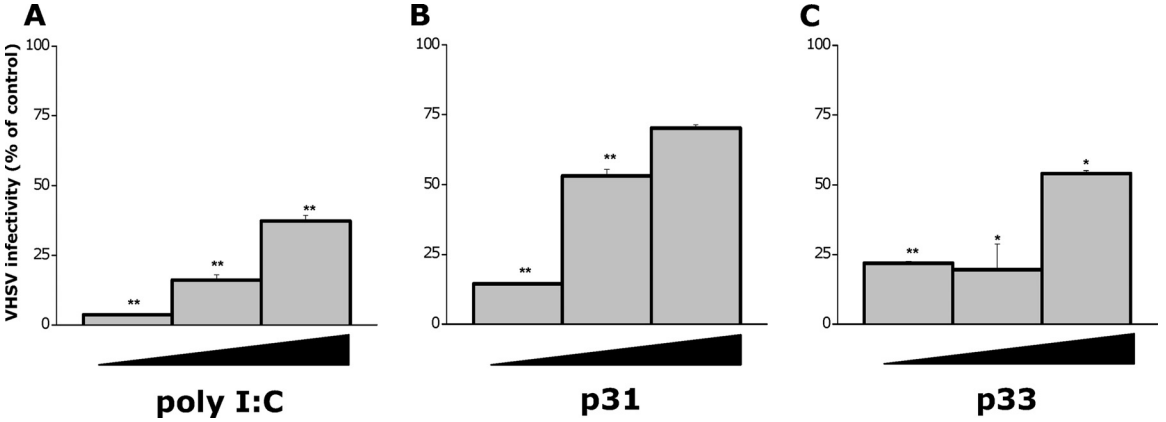

FIG. 6. Resistance to VHSV infection of RTG-2 cells treated with conditioned medium (CM) prepared from RTG-2 cells treated with the *mx3*-inducing peptides. RTG-2 cells were incubated for 24 h with increasing dilutions (1/5, 1/25, and 1/125) of CM prepared from cells treated with poly(I:C) (A), p31 (B), or p33 (C) and then infected with VHSV. Twenty-four hours after infection, VHSV infectivity was estimated by RT-qPCR. Black triangles represent increasing CM dilutions. The results are expressed as percentages of infectivity and calculated by the formula (VHSV infectivity in CM-treated cells/VHSV infectivity in nontreated cells) × 100. Data are the mean percentages of infectivity ± SD for two independent experiments, each performed in triplicate. Asterisks indicate significant differences in VHSV infectivity relative to the level for control cells at *P* values of <0.05 (*) and *P* values of <0.01 (**).

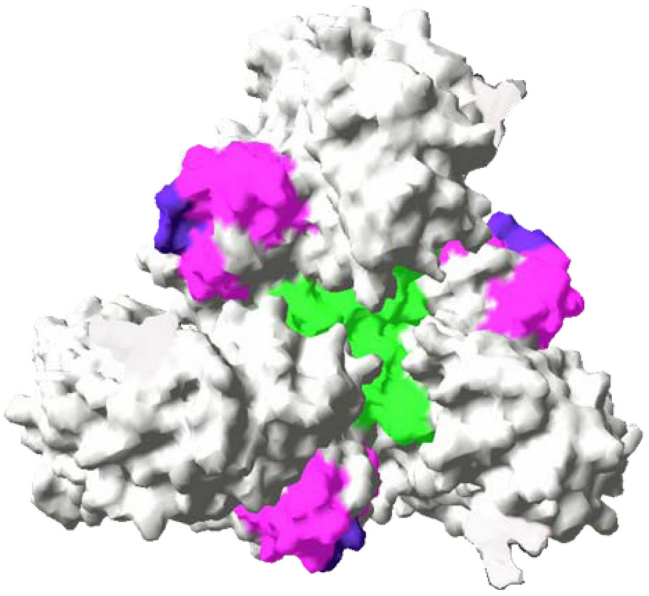

FIG. 7. gpG major *mx3*-inducing regions mapped onto the surface of the prefusion conformation of the VHSV gpG trimer (viewed looking down toward the membrane). Homology modeling for prediction of the 3D structure of VHSV gpG was carried out as indicated in Materials and Methods, using the prefusion conformation of VSV gpG (PDB file code 2J6J) as a template structure. Green, p31 (residues 280 to 310); magenta, p33 (residues 340 to 370); purple, RGD motif (residues 356 to 358).

case, a maximal reduction of VHSV infectivity of ~30% was observed at a CM dilution of 1/5 (data not shown). Since heat and acid treatments of gpG VHSV peptide-treated RTG-2 cells did not eliminate the anti-VHSV activity of these cells, the presence of type I IFN in supernatants from RTG-2 cells treated with gpG-VHSV-*mx3*-inducing peptides is confirmed.

DISCUSSION

Many studies have demonstrated that the protection afforded by the VHSV DNA vaccine correlated with the ability of VHSV gpG to induce a strong type I IFN-related immune response (19, 59). However, the precise mechanisms involved in this process remain largely unknown. In this study, we have focused on identifying the lineal determinants of VHSV gpG implicated in triggering the early events of the host innate immune response. The results obtained raised the possibility of the participation of at least two short lineal regions (amino acid residues 280 to 310 and 340 to 370) of this protein (Fig. 7) in the establishment of a functional type I IFN-mediated antiviral response.

First, to further establish the role of the gpG protein in the induction of type I IFN in the absence of other viral components, a cell line enriched in cells stably expressing gpG of VHSV on the membrane was generated (Fig. 1), and the IFN response was evaluated as the induction of the IS *mx3* gene elicited by those cells in the RTG-2 cells analyzed. As expected, potent *mx3* gene induction was achieved by fixed EPC-gpG cells expressing surface gpG (Fig. 2), as had already been described for other viruses (68), including HSV (13, 17, 45, 62), dengue virus (44), TGEV (17), HPIV-4A (42), and influenza virus (56).

Next, to identify the major lineal determinants of the gpG protein of VHSV implicated in triggering the IFN-mediated antiviral response, we used a pepscan methodology previously developed for mapping the domains of VHSV gpG implicated in VHSV-mediated membrane fusion (26, 58) as well as in host anamnesis immune response to VHSV infections (50, 51). This methodology is based on synthesizing a set of overlapping peptides (pepscan) spanning the entire sequence of gpG of $VHSV_{07.71}$ and then assaying each of the peptides for a defined activity/response, in this case for triggering the type I IFN-mediated antiviral response. Although the whole outer membrane domain of viral gp's had been considered essential for mediation of IFN induction (3, 17), our study showed that short protein segments of VHSV gpG are able to increase severalfold the basal expression level of the *mx3* gene (Fig. 4 and 5). However, this increment was always lower than the one induced by the gpG protein present in the membranes of fixed EPC-gpG cells (Fig. 1). The difference in relative activity between membrane-bound VHSV gpG and gpG peptides suggests that although the contact between gpG peptides and the cell surface receptor(s) can elicit the IFN response, other protein segments and/or the native conformation of the *mx3*-inducing peptides within the context of the entire protein must also contribute to the overall induction of the host antiviral responses to gpG. Similarly, recombinant forms of gp120 from R5 and X4 strains of HIV-1 were *per se* sufficient to induce clear-cut IFN secretion in plasmacytoid dendritic cells, although to a lesser extent than what was observed for the protein present on the surface of whole inactivated virus (25).

With respect to the *mx3*-inducing region spanning residues 280 to 310 of gpG, it is interesting to point out that this region included the sequence of the main domain of VHSV gpG inducing anamnestic trout leukocyte proliferation (residues 299 to 313) (50, 51), thus suggesting that this VHSV gpG *mx3*-inducing region might also act as a subdominant T-cell epitope detectable after DNA immunization and infection in fish. Alternatively, this result might confirm previous data showing that fish immunization with a plasmid encoding VHSV gpG induces a memory state in fish that, contrary to what would occur in mammals, primes the nonspecific immune responses upon a later encounter with the virus (22). Accordingly, type I IFN might also play an important role in the late specific stage of fish protection against virus.

The major *mx3*-inducing region located at residues 340 to 470 of VHSV gpG included an RGD motif (the sequence of a functional domain related to integrin binding) of certain importance in the *mx3* gene induction (Fig. 4). This, along with other data, for example, the presence of 2 RGD motifs in the gpG sequences of other fish rhabdoviruses, such as spring viremia carp virus (SVCV), and the existence of virion-associated cellular integrins (57) in VSV, suggests that rhabdovirus might interact with the integrins present on the surfaces of target cells, and this interaction might play a key role in triggering the host innate response observed after rhabdovirus infections. In any case, the fact that the RGD motif of VHSV gpG (residues 356 to 358) aligned with rabies virus (RV) gpG minor antigenic site a (amino acids 340 to 342) and VSV antigenic site B (amino acids 341 to 347) (64) seems to indicate

that this domain of the rhabdovirus gpG protein might be involved in the development of the host immune response. However, further studies involving the gpG sequences of other fish and mammalian rhabdoviruses are needed to corroborate this hypothesis. On the other hand, although no connection between integrins and IFN production in fish has yet been established, regulation of the expression of different IFN types by integrins in human immune (9) and nonimmune (40) cells has been demonstrated.

Finally, the fact that p9 (the peptide spanning the N-terminal segment of VHSV gpG, mapped by pepscan) failed to induce *mx3* gene expression might be explained by its internal position in the protein, since this region is implicated in some of the viral cell fusion events in VHSV (27) that, as for all rhabdoviruses (23, 34), is gpG mediated and occurs at acid pH in the endosomal compartment. Accordingly, this VHSV gpG protein region should not be accessible for interaction with the surface cell receptors sensed by viral gp's at physiological pH.

As stated before, IFN induction by viral gp's appears to result from an interaction of the viral gp's with the surfaces of the IFN-producing cells (30, 32). In this respect, after gpG binds to its cellular receptor(s), the major *mx*3-inducing regions of VHSV gpG, both of which are exposed at the top of the gpG molecule (Fig. 7), according to the prefusion three-dimensional structure of the VSV gpG ectodomain (63, 64), might be positioned close to the cell membrane for interacting with a specific secondary receptor(s), perhaps the integrins. We suggest that it is the latter interaction which triggers the IFN-mediated response. However, further studies are needed to characterize the cell signal pathway triggered by the rhabdovirus gpGs for inducing type I IFN-mediated antiviral responses.

ACKNOWLEDGMENTS

Thanks are due to Beatriz Bonmati for technical assistance.

This work was supported by projects AGL2008-03519-C04 and CSD2007-00002 (Consolider Ingenio 2010), both from MICINN (Spain).

REFERENCES

1. **Acosta, F., B. Collet, N. Lorenzen, and A. E. Ellis.** 2006. Expression of the glycoprotein of viral haemorrhagic septicaemia virus (VHSV) on the surface of the fish cell line RTG-P1 induces type 1 interferon expression in neighbouring cells. Fish Shellfish Immunol. **21:**272–278.
2. **Ankel, A., M. R. Capobianchi, C. Castilleti, and F. Dianzani.** 1994. Interferon induction by HIV glycoprotein 120: role of the V3 loop. Virology **205:**34–43.
3. **Ankel, H., D. F. Westra, S. Welling-Wester, and P. Lebon.** 1998. Induction of interferon-alpha by glycoprotein D of herpes simplex virus: a possible role of chemokine receptors. Virology **251:**317–326.
4. **Basurco, B., and J. M. Coll.** 1989. Spanish isolates and reference strains of viral haemorrhagic septicaemia virus shown similar protein size patterns. Bull. Eur. Assoc. Fish Pathol. **9:**92–95.
5. **Bazzigher, L., J. Pavlovic, O. Haller, and P. Staeheli.** 1992. Mx genes show weaker primary response to virus than other interferon-regulated genes. Virology **186:**154–160.
6. **Bearzotti, M., B. Delmas, A. Lamoureux, A. M. Loustau, S. Chilmonczyk, and M. Bremont.** 1999. Fish rhabdovirus cell entry is mediated by fibronectin. J. Virol. **73:**7703–7709.
7. **Bearzotti, M., A. F. Monnier, P. Vende, J. Grosclaude, P. DeKinkelin, and A. Benmansour.** 1995. The glycoprotein of viral hemorrhagic septicemia virus (VHSV): antigenicity and role in virulence. Vet. Res. **26:**413–422.
8. **Boehme, K. W., J. Singh, S. T. Perry, and T. Compton.** 2004. Human cytomegalovirus elicits a coordinated cellular antiviral response via envelope glycoprotein B. J. Virol. **78:**1202–1211.
9. **Boisvert, M., S. Gendron, N. Chetoui, and F. Aoudjit.** 2007. Alpha2 beta1 integrin signaling augments T cell receptor-dependent production of interferon-gamma in human T cells. Mol. Immunol. **44:**3732–3740.
10. **Boudinot, P., M. Blanco, P. de Kinkelin, and A. Benmansour.** 1998. Combined DNA immunization with the glycoprotein gene of viral hemorrhagic septicemia virus and infectious hematopoietic necrosis virus induces double-specific protective immunity and nonspecific response in rainbow trout. Virology **249:**297–306.
11. **Boyle, K. A., R. L. Pietropaolo, and T. Compton.** 1999. Engagement of the cellular receptor for glycoprotein B of human cytomegalovirus activates the interferon-responsive pathway. Mol. Cell. Biol. **19:**3607–3613.
12. **Brocal, I., A. Falco, V. Mas, A. Rocha, L. Perez, J. M. Coll, and A. Estepa.** 2006. Stable expression of bioactive recombinant pleurocidin in a fish cell line. Appl. Microbiol. Biotechnol. **72:**1217–1228.
13. **Capobianchi, M. R., J. Facchini, P. Di Marco, G. Antonelli, and F. Dianzani.** 1985. Induction of alpha interferon by membrane interaction between viral surface and peripheral blood mononuclear cells. Proc. Soc. Exp. Biol. Med. **178:**551–556.
14. **Carneiro, F. A., P. A. Lapido-Loureiro, S. M. Cordo, F. Stauffer, G. Weissmuller, M. L. Bianconi, M. A. Juliano, L. Juliano, P. M. Bisch, and A. T. Poian.** 2006. Probing the interaction between vesicular stomatitis virus and phosphatidylserine. Eur. Biophys. J. **35:**145–154.
15. **Cole, A. M., P. Weis, and G. Diamond.** 1997. Isolation and characterization of pleurocidin, an antimicrobial peptide in the skin secretions of winter flounder. J. Biol. Chem. **272:**12008–12013.
16. **Cseke, G., M. S. Maginnis, R. G. Cox, S. J. Tollefson, A. B. Podsiad, D. W. Wright, T. S. Dermody, and J. V. Williams.** 2009. Integrin alphavbeta1 promotes infection by human metapneumovirus. Proc. Natl. Acad. Sci. U. S. A. **106:**1566–1571.
17. **Charley, B., and H. Laude.** 1988. Induction of alpha interferon by transmissible gastroenteritis coronavirus: role of transmembrane glycoprotein E1. J. Virol. **62:**8–11.
18. **Chico, V., N. Gomez, A. Estepa, and L. Perez.** 2006. Rapid detection and quantitation of viral hemorrhagic septicemia virus in experimentally challenged rainbow trout by real-time RT-PCR. J. Virol. Methods **132:**154–159.
19. **Chico, V., M. Ortega-Villaizan, A. Falco, C. Tafalla, L. Perez, J. Coll, and A. Estepa.** 2009. The immunogenicity of viral haemorragic septicaemia rhabdovirus (VHSV) DNA vaccines can depend on plasmid regulatory sequences. Vaccine **27**(13)**:**1938–1948.
20. Reference deleted.
21. **Chiou, P., J. Khoo, N. C. Bols, S. Douglas, and T. T. Chen.** 2006. Effects of linear cationic alpha-helical antimicrobial peptides on immune-relevant genes in trout macrophages. Dev. Comp. Immunol. **30:**797–806.
22. **Cuesta, A., and C. Tafalla.** 2009. Transcription of immune genes upon challenge with viral hemorrhagic septicemia virus (VHSV) in DNA vaccinated rainbow trout (Oncorhynchus mykiss). Vaccine **27:**280–289.
23. **Da Poian, A. T., F. A. Carneiro, and F. Stauffer.** 2005. Viral membrane fusion: is glycoprotein G of rhabdoviruses a representative of a new class of viral fusion proteins? Braz. J. Med. Biol. Res. **38:**813–823.
24. **DeKinkelin, P., and M. LeBerre.** 1977. Isolament d'un rhabdovirus pathogéne de la truite fario (Salmo trutta, L. 1766). C. R. Acad. Sci. Paris **284:** 101–104.
25. **Del Cornò, M., M. C. Gauzzi, G. Penna, F. Belardelli, L. Adorini, and S. Gessani.** 2005. Human immunodeficiency virus type 1 gp120 and other activation stimuli are highly effective in triggering alpha interferon and CC chemokine production in circulating plasmacytoid but not myeloid dendritic cells. J. Virol. **79:**12597–12601.
26. **Estepa, A., and J. M. Coll.** 1996. Pepscan mapping and fusion-related properties of the major phosphatidylserine-binding domain of the glycoprotein of viral hemorrhagic septicemia virus, a salmonid rhabdovirus. Virology **216:** 60–70.
27. **Estepa, A., A. Rocha, L. Pérez, J. A. Encinar, E. Nuñez, A. Fernandez, J. M. Gonzalez Ros, F. Gavilanes, and J. M. Coll.** 2001. A protein fragment from the salmonid VHS rhabdovirus induces cell-to-cell fusion and membrane phosphatidylserine translocation at low pH. J. Biol. Chem. **276:**46268–46275.
28. **Falco, A., V. Chico, L. Marroqui, L. Perez, J. M. Coll, and A. Estepa.** 2008. Expression and antiviral activity of a beta-defensin like peptide identified in the rainbow trout (Oncorhynchus mykiss) EST sequences. Mol. Immunol. **45:**757–765.
29. **Falco, A., V. Mas, C. Tafalla, L. Perez, J. M. Coll, and A. Estepa.** 2007. Dual antiviral activity of human alpha-defensin-1 against viral haemorrhagic septicaemia rhabdovirus (VHSV): inactivation of virus particles and induction of a type I interferon-related response. Antiviral Res. **76:**111–123.
30. **Feldman, S. B., M. Ferraro, H. M. Zheng, N. Patel, S. Gould-Fogerite, and P. Fitzgerald-Bocarsly.** 1994. Viral induction of low frequency interferon-alpha producing cells. Virology **204:**1–7.
31. **Fijan, N., D. Sulimanovic, M. Bearzotti, D. Mizinic, L. O. Zwillenberg, S. Chilmonczyk, J. F. Vautherot, and P. de Kinkelin.** 1983. Some properties of the Epithelioma papulosum cyprini (EPC) cell line from carp Cyprinus carpio. Ann. Virol. **134:**207–220.
32. **Fitzgerald-Bocarsly, P.** 1993. Human natural interferon-alpha producing cells. Pharmacol. Ther. **60:**39–62.
33. **Garcia, M. A., E. F. Meurs, and M. Esteban.** 2007. The dsRNA protein kinase PKR: virus and cell control. Biochimie **89:**799–811.
34. **Gaudin, Y.** 2000. Reversibility in fusion protein conformational changes. The

intriguing case of rhabdovirus-induced membrane fusion. Subcell. Biochem. **34:**379–408.
35. **Gaudin, Y., P. DeKinkelin, and A. Benmansour.** 1999. Mutations in the glycoprotein of viral haemorrhagic septicaemia virus that affect virulence for fish and the pH threshold for membrane fusion. J. Gen. Virol. **80:**1221–1229.
36. **Georgel, P., Z. Jiang, S. Kunz, E. Janssen, J. Mols, K. Hoebe, S. Bahram, M. Oldstone, and B. Beutler.** 2007. Vesicular stomatitis virus glycoprotein G activates a specific antiviral Toll-like receptor 4-dependent pathway. Virology **362**(2)**:**304–313.
37. **Ghosh, S. K., J. Kusari, S. K. Bandyopadhyay, H. Samanta, R. Kumar, and G. C. Sen.** 1991. Cloning, sequencing, and expression of two murine 2′-5′-oligoadenylate synthetases. Structure-function relationships. J. Biol. Chem. **266:**15293–15299.
38. **Haller, O., P. Staeheli, and G. Kochs.** 2007. Interferon-induced Mx proteins in antiviral host defense. Biochimie **89:**812–818.
39. **Halminen, M., J. Ilonen, I. Julkunen, O. Ruuskanen, O. Simell, and M. J. Makela.** 1997. Expression of MxA protein in blood lymphocytes discriminates between viral and bacterial infections in febrile children. Pediatr. Res. **41:**647–650.
40. **Higuchi, A., Y. Takanashi, N. Tsuzuki, T. Asakura, C. S. Cho, T. Akaike, and M. Hara.** 2003. Production of interferon-beta by fibroblast cells on membranes prepared with RGD-containing peptides. J. Biomed. Mater. Res. A **65**(3)**:**369–378.
41. **Hovanessian, A. G., and J. Justesen.** 2007. The human 2′-5′oligoadenylate synthetase family: unique interferon-inducible enzymes catalyzing 2′-5′ instead of 3′-5′ phosphodiester bond formation. Biochimie **89:**779–788.
42. **Ito, Y., H. Bando, H. Komada, M. Tsurudome, M. Nishio, M. Kawano, H. Matsumura, S. Kusagawa, T. Yuasa, and H. Ohta.** 1994. HN proteins of human parainfluenza type 4A virus expressed in cell lines transfected with a cloned cDNA have an ability to induce interferon in mouse spleen cells. J. Gen. Virol. **75:**567–572.
43. **Kim, C. H., M. C. Johnson, J. D. Drennan, B. E. Simon, E. Thomann, and J. A. Leong.** 2000. DNA vaccines encoding viral glycoproteins induce nonspecific immunity and Mx protein synthesis in fish. J. Virol. **74:**7048–7054.
44. **Kurane, I., A. Meager, and F. A. Ennis.** 1986. Induction of interferon alpha and gamma from human lymphocytes by dengue virus-infected cells. J. Gen. Virol. **67**(8)**:**1653–1661.
45. **Lebon, P., M. J. Commoy-Chevalier, B. Robert-Galliot, A. Morin, and C. Chany.** 1980. Production of human type I interferon by lymphocytes in contact with cells infected by herpesvirus and fixed with glutaraldehyde. C. R. Seances Acad. Sci. D **290:**37–40. (In French.)
46. **Livak, K. J., and T. D. Schmittgen.** 2001. Analysis of relative gene expression data using real-time quantitative PCR and the 2(-Delta Delta C(T)) method. Methods **25:**402–408.
47. **Lorenzen, N., E. Lorenzen, K. Einer-Jensen, and S. E. LaPatra.** 2002. DNA vaccines as a tool for analysing the protective immune response against rhabdoviruses in rainbow trout. Fish Shellfish Immunol. **12:**439–453.
48. **Lorenzen, N., E. Lorenzen, K. Einer-Jensen, and S. E. LaPatra.** 2002. Immunity induced shortly after DNA vaccination of rainbow trout against rhabdoviruses protects against heterologous virus but not against bacterial pathogens. Dev. Comp. Immunol. **26:**173–179.
49. **Lorenzo, G., A. Estepa, and J. M. Coll.** 1996. Fast neutralization/immunoperoxidase assay for viral haemorrhagic septicemia with anti-nucleoprotein monoclonal antibody. J. Virol. Methods **58:**1–6.
50. **Lorenzo, G., A. Estepa, S. Chilmonczyk, and J. M. Coll.** 1995. Mapping of the G and N regions of viral haemorrhagic septicemia virus (VHSV) inducing lymphoproliferation by pepscan. Vet. Res. **26:**521–525.
51. **Lorenzo, G. A., A. Estepa, S. Chilmonczyk, and J. M. Coll.** 1995. Different peptides from haemorrhagic septicemia rhabdoviral proteins stimulate leucocyte proliferation with individual fish variation. Virology **212:**348–355.
52. **Mas, V., L. Perez, J. A. Encinar, M. T. Pastor, A. Rocha, E. Perez-Paya, A. Ferrer-Montiel, J. M. Gonzalez Ros, A. Estepa, and J. M. Coll.** 2002. Salmonid viral haemorrhagic septicaemia virus: fusion-related enhancement of virus infectivity by peptides derived from viral glycoprotein G or a combinatorial library. J. Gen. Virol. **83:**2671–2681.
53. **Mas, V., A. Rocha, L. Perez, J. M. Coll, and A. Estepa.** 2004. Reversible inhibition of spreading of in vitro infection and imbalance of viral protein accumulation at low pH in viral hemorrhagic septicemia rhabdovirus, a salmonid rhabdovirus. J. Virol. **78:**1936–1944.
54. **McFadden, G., R. M. Mohamed, M. M. Rahman, and E. Bartee.** 2009. Cytokine determinants of viral tropism. Nat. Rev. Immunol. **9:**645–656.
55. **McLauchlan, P. E., B. Collet, E. Ingerslev, C. J. Secombes, N. Lorenzen, and A. E. Ellis.** 2003. DNA vaccination against viral haemorrhagic septicaemia (VHS) in rainbow trout: size, dose, route of injection and duration of protection-early protection correlates with Mx expression. Fish Shellfish Immunol. **15:**39–50.
56. **Miller, J. L., and E. M. Anders.** 2003. Virus-cell interactions in the induction of type 1 interferon by influenza virus in mouse spleen cells. J. Gen. Virol. **84:**193–2002.
57. **Moerdyk-Schauwecker, M., S. Hwang, and V. Z. Grdzelishvili.** 2009. Analysis of virion associated host proteins in vesicular stomatitis virus using a proteomics approach. Virol. J. **6:**166.
58. **Nunez, E., A. M. Fernandez, A. Estepa, J. M. Gonzalez-Ros, F. Gavilanes, and J. M. Coll.** 1998. Phospholipid interactions of a peptide from the fusion-related domain of the glycoprotein of VHSV, a fish rhabdovirus. Virology **243:**322–330.
59. **Purcell, M. K., K. M. Nichols, J. R. Winton, G. Kurath, G. H. Thorgaard, P. Wheeler, J. D. Hansen, R. P. Herwig, and L. K. Park.** 2006. Comprehensive gene expression profiling following DNA vaccination of rainbow trout against infectious hematopoietic necrosis virus. Mol. Immunol. **43:**2089–2106.
60. **Raida, M. K., and K. Buchmann.** 2008. Bath vaccination of rainbow trout (Oncorhynchus mykiss Walbaum) against Yersinia ruckeri: effects of temperature on protection and gene expression. Vaccine **26:**1050–1062.
61. **Randall, R. E., and S. Goodbourn.** 2008. Interferons and viruses: an interplay between induction, signalling, antiviral responses and virus countermeasures. J. Gen. Virol. **89:**1–47.
62. **Reske, A., G. Pollara, C. Krummenacher, D. R. Katz, and B. M. Chain.** 2008. Glycoprotein-dependent and TLR2-independent innate immune recognition of herpes simplex virus-1 by dendritic cells. J. Immunol. **180:**7525–7536.
63. **Roche, S., S. Bressanelli, F. A. Rey, and Y. Gaudin.** 2006. Crystal structure of the low-pH form of the vesicular stomatitis virus glycoprotein G. Science **313:**187–191.
64. **Roche, S., F. A. Rey, Y. Gaudin, and S. Bressanelli.** 2007. Structure of the prefusion form of the vesicular stomatitis virus glycoprotein G. Science **315:**843–848.
65. **Ruoslahti, E.** 1996. RGD and other recognition sequences for integrins. Annu. Rev. Cell Dev. Biol. **12:**697–715.
66. **Saksela, E., I. Virtanen, T. Hovi, D. S. Secher, and K. Cantell.** 1984. Monocyte is the main producer of human leukocyte alpha interferons following Sendai virus induction. Prog. Med. Virol. **30:**78–86.
67. **Samuel, C. E.** 2001. Antiviral actions of interferons. Clin. Microbiol. Rev. **14:**778–809.
68. **Seeds, R. E., S. Gordon, and J. L. Miller.** 2006. Receptors and ligands involved in viral induction of type I interferon production by plasmacytoid dendritic cells. Immunobiology **211:**525–535.
69. **Simon, A., J. Fah, O. Haller, and P. Staeheli.** 1991. Interferon-regulated Mx genes are not responsive to interleukin-1, tumor necrosis factor, and other cytokines. J. Virol. **65:**968–971.
70. **Staeheli, P., F. Pitossi, and J. Pavlovic.** 1993. Mx proteins: GTPases with antiviral activity. Trends Cell Biol. **3:**268–272.
71. **Stark, G. R., I. M. Kerr, B. R. G. Williams, R. H. Silverman, and R. D. Schreiber.** 1998. How cells respond to interferons. Annu. Rev. Biochem. **67:**227–264.
72. **Stetson, D. B., and R. Medzhitov.** 2006. Antiviral defense: interferons and beyond. J. Exp. Med. **203:**1837–1841.
73. **Tafalla, C., V. Chico, L. Perez, J. M. Coll, and A. Estepa.** 2007. In vitro and in vivo differential expression of rainbow trout (Oncorhynchus mykiss) Mx isoforms in response to viral haemorrhagic septicaemia virus (VHSV) G gene, poly I:C and VHSV. Fish Shellfish Immunol. **23:**210–221.
74. **Thiry, M., F. Lecoq-Xhonneux, I. Dheur, A. Renard, and D. Kinkelin.** 1990. Molecular cloning of the m-RNA coding for the G protein of the viral haemorrhagic septicaemia (VHS) of salmonids. J. Vet. Microbiol. **23:**221–226.
75. **Thiry, M., F. Lecoq-Xhonneux, I. Dheur, A. Renard, and D. Kinkelin.** 1991. Sequence of a cDNA carrying the glycoprotein gene and part of the matrix protein M2 gene of viral haemorrhagic septicaemia virus, a fish rhabdovirus. Biochim. Biophys. Acta **1090:**345–347.
76. **Thompson, J. D., D. G. Higgins, and T. J. Gibson.** 1994. CLUSTAL W: improving the sensitivity of progressive multiple sequence alignment through sequence weighting, position-specific gap penalties and weight matrix choice. Nucleic Acids Res. **22:**4673–4680.
77. **Verjan, N., E. L. Ooi, T. Nochi, H. Kondo, I. Hirono, T. Aoki, H. Kiyono, and Y. Yuki.** 2008. A soluble nonglycosylated recombinant infectious hematopoietic necrosis virus (IHNV) G-protein induces IFNs in rainbow trout (Oncorhynchus mykiss). Fish Shellfish Immunol. **25:**170–180.
78. **Villard, V., O. Kalyuzhniy, O. Riccio, S. Potekhin, T. N. Melnik, A. V. Kajava, C. Ruegg, and G. Corradin.** 2006. Synthetic RGD-containing alpha-helical coiled coil peptides promote integrin-dependent cell adhesion. J. Pept. Sci. **12:**206–212.
79. **von Wussow, P., D. Jakschies, H. K. Hochkeppel, C. Fibich, L. Penner, and H. Deicher.** 1990. The human intracellular Mx-homologous protein is specifically induced by type I interferons. Eur. J. Immunol. **20:**2015–2019.
80. **Wolf, F., and M. C. Quimby.** 1962. Established eurythermic line of fish cells in vitro. Science **135:**1065–1066.
81. **Zou, J., C. Tafalla, J. Truckle, and C. J. Secombes.** 2007. Identification of a second group of type I IFNs in fish sheds light on IFN evolution in vertebrates. J. Immunol. **179:**3859–3871.